Antiferromagnetic ordering in a 90 K copper oxide superconductor.

J.A. Hodges¹, Y. Sidis², P. Bourges², I. Mirebeau², M. Hennion² and X. Chaud³.

¹DRECAM-SPEC, CE-Saclay, 91191 Gif sur Yvette, France.

² Laboratoire Léon Brillouin, CEA-CNRS, CE-Saclay, 91191 Gif sur Yvette, France.

³CRETA, CNRS, 25 Avenue des Martyrs, BP 166 38042 Grenoble cedex, France.

(October 31, 2018)

Using elastic neutron scattering, we evidence a commensurate antiferromagnetic Cu(2) order (AF) in the superconducting (SC) high- T_c cuprate $YBa_2(Cu_{1-y}Co_y)_3O_{7+\delta}$ (y=0.013, T_c =93 K). However, the spin excitation spectrum is still dominated by a magnetic resonance peak at 41 meV as in the Co-free system, but with a reduced spectral weight. The substitution of Co thus leads to a state where AF and SC cohabit. These results show that the hole-doped CuO_2 plane is close to an AF instability even when T_c remains optimum.

The interplay between magnetic order and superconductivity is an interesting and profound phenomenon ubiquitous in strongly correlated systems, such as high- T_c cuprates, low- T_c ruthenates and heavy fermions There have been a number of reports of the coexistence of magnetic order and exotic superconductivity: for example, in Ce and U-based heavy fermion systems [1,2], in superoxygenated La₂CuO_{4+ δ}, in $La_{1.6-x}Nd_{0.4}Sr_xCuO_4$ [3,4] and more recently in the well underdoped regime of $YBa_2Cu_3O_{6+x}$ (x=0.5-0.6) [5,6]. In the last case [6], the observation that the magnetic intensity decreases at large momentum more rapidly than does the Cu-spin form factor, has been considered to support the suggestion of orbital moments of a d-wave density-wave (DDW) order parameter (that could be the hidden order responsible for the "pseudo-gap phase" of underdoped cuprates) [7]. However, in the cuprates, the real coexistence of magnetic order and superconductivity or a microscopic phase segregation remains a matter of discussion. Especially, the role played by disorder is still an open question [8]. In this letter, we evidence the appearance of antiferromagnetic order in the CuO₂ planes of a fully oxydised superconducting YBa₂Cu₃O₇ based system with $T_c=93$ K, when a disorder is introduced through the substitution of cobalt atoms at the copper site of the chains.

The YBa₂Cu₃O_{6+x} perovskite structure contains two copper sites: Cu(1) belonging to the Cu-O chains (along the **b**-axis), and Cu(2) belonging to the CuO₂ planes. Co³⁺ ions substitute only at the Cu(1) sites [9]. Due to its higher oxidation state compared to that of Cu(1), the Co cation pulls in extra oxygen to increase its oxygen-coordination. Each added Co atom, with an average coordination number of 5, pulls in 0.5 oxygen atoms [9–12]. Additionally, the Co substitution induces a transverse distortion of its Cu(1) site [11,12]. Co atoms tend to form either small clusters like dimers [9,12] or even short chains along the (110) direction [11]. As a result, these chains pin down the twin boundaries of the orthorhombic structure (micro-twinning) that triggers an

orthorhombic-tetragonal transition for $y \ge 0.025$ [13]. NMR [14] and transport measurements [15] show the cobalt substitution reduces the hole doping. However, for the low Co substitution level ($y \simeq 0.013$) examined here, despite the decrease in the Hall effect derived carrier density [15] and in the specific heat derived condensate density [16], the doping is still high enough for T_c to remain at its optimum value. In addition, Nuclear Quadrupole Resonance (NQR) [17] measurements have evidenced the appearance of magnetic moments on the Cu of the Cu(1) sites and more surprisingly on those of the Cu(2) sites as well. Mössbauer probe measurements [18] have also evidenced the moments on the Cu(2) sites.

We present a neutron scattering study of the magnetic properties of a large single crystal (1.4 cm³) of fully oxygenated YBa₂(Cu_{1-y}Co_y)₃O_{7+ δ}. The sample was prepared by the top-seed melt texturing method. A microprobe analysis confirmed the Co content was that of the starting mixture, y=0.013, and showed the Co was uniformly distributed on the μ m scale. Neutron depolarization measurements (Fig 3.c) provided T_c= 93 K.

The neutron scattering experiments were performed on the triple axis spectrometers 1T1 and 4F2 at the Laboratoire Léon Brillouin, Saclay (France). For elastic neutron scattering measurements (ENS) on 4F2, double PG(002) monochromators and analyzer were used and a beryllium filter was inserted into the scattered beam in order to remove higher order contamination. The data were taken with a fixed final wavevector of 1.55 $Å^{-1}$. For the inelastic neutron scattering measurements (INS) on 1T1, a focusing Cu(110) monochromator and a PG(002) analyzer were used and a pyrolytic graphite filter was inserted into the scattered beam. The data were taken with a fixed final wavevector of 4.1 Å^{-1} . Measurements were carried out with the crystal in two different orientations where wave vector transfers of the form $\mathbf{Q}=(H, H, L)$ and (3H, H, L), respectively, were accessible. Throughout this article, the wave vector \mathbf{Q} is indexed in units of the reciprocal tetragonal lattice vectors $2\pi/a=2\pi/b=1.63 \text{ Å}^{-1}$ and $2\pi/c=0.53 \text{ Å}^{-1}$. In this notation the $(\pi/a, \pi/a)$ wave

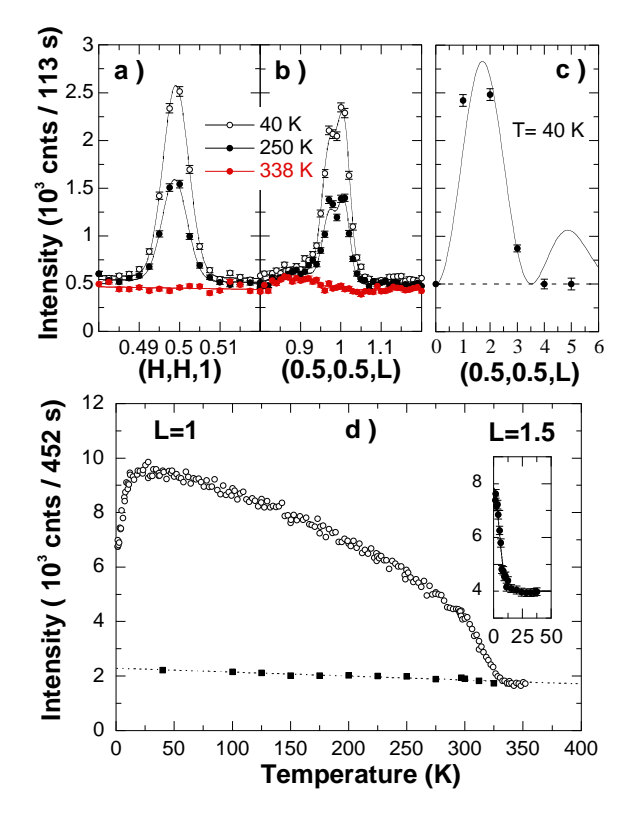


FIG. 1. Elastic neutron intensity along a) the (110) direction and b) the (001) direction around $\mathbf{Q}=(0.5,0.5,1)$. c) L-dependence of magnetic intensity at different AF peaks, $\mathbf{Q}=(0.5,0.5,\mathrm{L})$. The full line represents the magnetic intensity expected from in-plane Cu(2) spins with isotropic Cu²⁺ form factor and including the resolution correction. d) Temperature dependences of the neutron scattering intensity at $\mathbf{Q}=(0.5,0.5,1)$. The full squares represent the background from scans as shown in a) and b). Inset of d) shows the appearance of magnetic intensity at $\mathbf{Q}=(0.5,0.5,1.5)$ below $T_m \simeq 12$ K where the peak at $\mathbf{Q}=(0.5,0.5,1)$ displays a re-entrant behavior.

vector parallel to the CuO_2 planes corresponds to points of the form (h/2,k/2) with h and k odd integers.

We first describe the observation of the commensurate magnetic order. Figure 1 shows the elastic neutron intensity at the antiferromagnetic wavevector $\mathbf{Q}=(0.5,0.5,1)$ along both the (110) and (001) directions. The peak, absent at 338 K and present at 250 K and 40 K, evidences the magnetic order. Different antiferromagnetic peaks, $\mathbf{Q}=(0.5,0.5,\mathrm{L})$ with L integer, are reported in Fig. 1.c where magnetic intensity is sizeable at L=1,2,3. The observed pattern (Fig. 1.c) and the absence of any magnetic peak at $\mathbf{Q}=(0.5,0.5,0)$ implies that the magnetic response is fully dominated by magnetic moments at the Cu(2) sites. Assuming all of the Cu(2) carry the same ordered moment, we obtain a low temperature (T=40 K) mean moment of $\sim 0.10 \pm 0.05 \mu_B$. Gaussian fits of Fig. 1 at different temperatures shows that the AF order is

resolution limited, meaning that the correlation lengths are typically $\xi > 200$ Å. A detailed q-dependence of the magnetic peak, see for instance the double peak structure of the scan along \mathbf{c}^* of Fig. 1.b, shows a mosaic distribution of the magnetic peak which does not exactly reproduce that of the nuclear peaks. This means that the volume of AF region does not exactly match the volume of the single crystal.

The temperature dependence of the neutron scattering intensity measured at the antiferromagnetic wavevector $\mathbf{Q}=(0.5,0.5,1)$ (Fig. 1.d) shows the system orders at $T_N \sim 330$ K. As the temperature is lowered, the AF Bragg intensity initially increases continuously and no anomaly is observed on passing through T_c . The peak intensity displays a marked downturn at $T_m \simeq 12$ K, and almost half of its intensity is left as $T \rightarrow 0$. Below T_m , additional neutron intensity occurs at L=1.5 indicating the system undergoes an AFI-AFII transition, characterized by the doubling of the AF unit cell along the c axis. This transition is also observed in YBa₂Cu₃O₆ when substituted at the Cu(1) site [19,20] and AFII ordering is observed in non-superconducting YBa₂(Cu_{1-v}Co_v)₃O_{7+δ} with high Co substitution levels [21]. The re-ordering observed in the present case may be linked to the influence of magnetic freezing which is known to exist in in similar samples, For example, in YBa₂(Cu_{0.94}Co_{0.06})₃O_{7+ δ}, time of flight neutron scattering measurements [22] have evidenced the progressive freezing of the Co moments as the temperature is lowered in agreement with local probe measurements [17,18].

Without producing any reduction in the superconducting transition temperature, the substitution of magnetic $\mathrm{Co^{3+}}$ at the chain sites thus introduces a very specific perturbation which induces a commensurate AF 3D order, below $\mathrm{T}_N \sim 330~\mathrm{K}$, at the copper sites of the $\mathrm{CuO_2}$ planes. A key question is how does the superconductivity and the antiferromagnetic order cohabit ?

To address this issue, we first consider the possibility of complete phase segregation, such that only a small fraction of Cu(2) atoms, for example those adjacent to a Co atom, carries the full magnetic moment of the undoped cuprates (0.6 μ_B). The concentration of Cu(2) atoms (in the planes) needed to account for the observed scattering intensity would then be $\sim 3\%$ which is roughly comparable to the Co substitution level (in the chains). There are a number of arguments against this hypothesis. As the magnetic correlation length exceeds 200 Å, then the Co would be essentially concentrated within these clusters. Such Co clusters would yield an observable magnetic diffraction pattern. The local Co concentration would also be quite high and we would expect to observe the behavior seen in samples having high Co levels. For example, insulating samples of $YBa_2(Cu_{1-v}(Co, Fe)_v)_3O_{7+\delta}$ show the AFII structure up to $T_N \sim 400 \text{ K} [19,21]$, whereas it is the AFI structure that is observed here at T_N . Neither of these features is observed. Further ar-

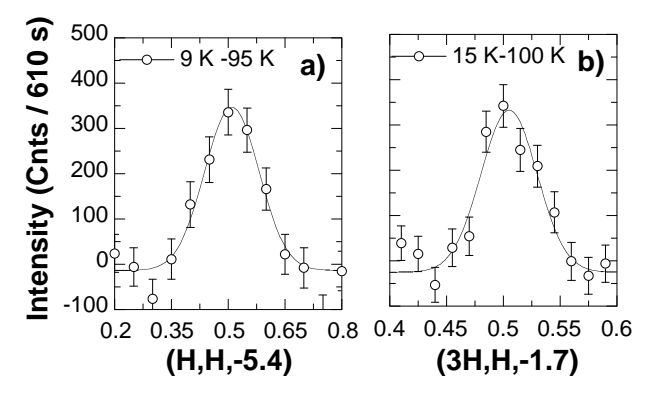


FIG. 2. Difference of constant energy scans performed at 39 meV measured at low temperature, and just above T_c : a) around \mathbf{Q} =(0.5,0.5,-5.4) along the (110) direction: b)around \mathbf{Q} =(1.5,0.5,-1.7) along the (310) direction. Solid lines are fit by Gaussian lineshape.

guments against complete phase separation is provided by Cu-NQR [17] or Y-NMR [14] local probe measurements in YBa₂(Cu_{1-y}Co_y)₃O_{7+ δ} which evidence features that are different from those of the undoped insulating AF state. We recall also that local probe Cu NQR [17] and Mössbauer [18] measurements on samples having the same low Co substitution level as the sample studied here have shown that over 50 % of the Cu(2) carry magnetic moments. Thus, it does not seem possible that the AF order could be linked to the existence of locally undoped regions. Consequently, the two phenomena (AF and SC) appear to be in contact at a microscopic level.

As the Co atoms aggregate into dimers or small clusters forming lines along the (110) direction [11], we speculate that these lines of magnetic Co atoms are the perturbing elements which induce the AF order into the CuO₂ planes. However, we recall the Cu(2) moments are not confined to the immediate vicinity of these lines for the magnetic correlation lengths greatly exceed the lateral dimensions of a twin boundary.

Finally, we believe this new AF order is analogous to that recently reported in underdoped YBa₂Cu₃O_{6+x} ($x \sim 0.5$ - 0.6) [5,6] with however one striking difference: the additional enhancement of the AF intensity observed below T_c is not seen in the present case. At large Q, the intensity decreases much more rapidly than expected for the Cu-spin form factor (see Fig. 1.c). This result is similar to that observed in well underdoped YBa₂Cu₃O_{6.6} [6] where it was interpreted as evidencing DDW order [7]. Our finding of a similar unusual structure factor in a Co-substituted sample which is near optimal doping and where a pseudo-gap behavior is absent, questions this conclusion. The precise reason for the observed structure factor remains unclear at present.

We next present the inelastic magnetic fluctuations around the AF wavevector. In cobalt-free optimally doped YBa₂Cu₃O_{7- δ}, the AF correlations are purely dy-

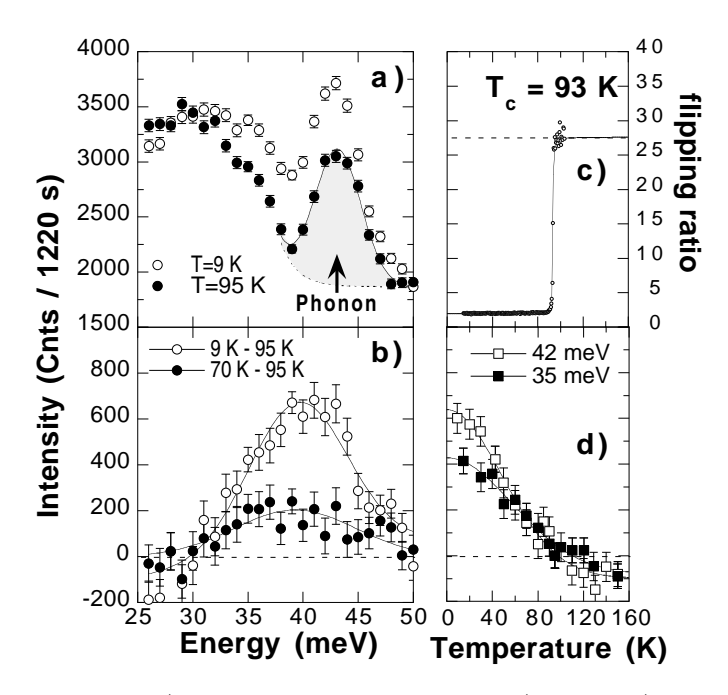


FIG. 3. a) Energy scans performed at \mathbf{Q} =(0.5,0.5,-5.4) at T=9.2 K and T=95 K. The scan above T_c looks very similar to that in the Co-free sample with the phonon peak at 42.5 meV [24]. b) Difference between energy scans performed at 9.2 K (or 70 K) and at 95 K. c) determination of $T_c=93$ K by the neutron depolarisation technique. d) temperature dependence of the AF response at 35 meV and 42 meV.

namic, and the spin excitation spectrum in the superconducting state is characterized by a sharp antiferromagnetic excitation peaked at 41 meV, the so-called "magnetic resonance peak" [23,24]. In our cobalt substituted sample, we looked for this magnetic excitation specific of d-wave superconductivity and we performed constant energy scans at 39 meV around Q=(0.5,0.5,-5.4) along the (110) direction as well as around (1.5,0.5,-1.7) along the (310) direction (Fig. 2). At low temperature, a peak shows up in both scans centered at the AF wave vector. The ratio of the intensity of both scans evolves as a function of Q as expected for the Cu²⁺ anisotropic magnetic form factor [20]. In both scans, the peak diminishes drastically at T_c. Above T_c, weaker intensity, peaked at AF wavevector, remains in both scans, in agreement with the Co-free compound YBa₂Cu₃O_{6.97} [24]. After subtraction of the scan just above T_c from that at low temperature, the remaining intensity was fitted to a Gaussian profile centered at the AF wave vector. For both types of constant energy scans reported in Fig. 2, the AF response at 39 meV in the superconducting state displays a momentum width (FWHM) of $0.28 \pm 0.06 \text{ Å}^{-1}$. This momentum distribution is similar to that of the magnetic resonance peak in the Co-free system [24].

Figure 3 shows energy scans performed at Q=(0.5,0.5,-5.4) at low temperature and just above T_c . The enhance-

ment of the AF response around 41 meV (the magnetic resonance peak) is visible in the raw data and it is further confirmed by the differences shown on Fig. 3.b. The magnetic resonance peak is not sharp in energy and can be fitted by the usual "ansatz" of a single Gaussian lineshape: this yields an intrinsic energy width of $\sim 9 \pm 1$ meV (FWHM). This analysis in terms of a single broad signal centered at E_r is supported by the temperature dependences performed at the AF wave vector at 42 meV and 35 meV (6 meV below E_r) which both show a similar decrease of the AF response up to T_c (Fig. 3.c). As a function of temperature, the magnetic resonance peak disappears at T_c without any significant shift of its characteristic energy (Fig. 3.b). Furthermore, its energy and momentum integrated intensity, calibrated in absolute unit against the phonon at 42.5 meV, is $\sim 0.025 \ \mu_{\rm B}^2$, i.e it is about twice weaker than that reported in the Co-free compound [25].

The spin dynamics observed following Co substitution (at the Cu(1) site) show some features which are common to those observed with Ni and Zn substitutions (at the Cu(2) site), where a broadened magnetic resonance peak was also seen [26]. However, the Ni and Zn substitutions have more drastic effects on the dynamical AF correlations: Zn already induces strong AF fluctuations in the normal state although it reduces the enhancement of the spin susceptibility in the SC state, whereas Ni renormalizes the resonance energy.

Following the observed 50% reduction in the weight of the resonance peak, it is possible that distinct superconducting regions occupy about half of the sample volume leaving the remainder for the distinct magnetically ordered regions. This fully agrees with NQR results on sample with similar Co content which show that about half the Cu(2) carry magnetic moments [17]. Such a phase segregation scenario has some analogies with the three phase model developed to explain the Cu-NQR data [17]. However, the magnetic correlation lengths found here $(\xi > 200\text{\AA})$ are much bigger than the dimensions of the nucleated regions where the Cu(2) become magnetic as considered in ref. [17]. In addition, Kohno et al. [8] have proposed a phenomenological description of AF-SC coexistent states due to disorder in strongly correlated systems. In their model, based on Ginsburg-Landau theory, a key assumption is that the SC state is in competition with the AF phase with a first order phase boundary, which enables the AF state to nucleate where SC is suppressed. For a finite concentration of impurities, the first order AF-SC boundary of the clean case is replaced by a finite region where the SC and AF moments coexist microscopically with spatially varying order parameters. It has also been proposed [27] that an AF state can locally appear around surfaces or impurities and can co-exist with d-wave superconductivity and in particular, the local formation of an AF order parameter can easily occur near a (110) surface. The AF order in the present

case could have its origin in the magnetic polarisation produced by the Co³⁺ or in the structural effects related to the micro-twinning along the (110) directions [13] or more probably, to a combination of both these effects.

As a conclusion, we observe a Cu(2) site commensurate long range AF order in the superconducting high- T_c cuprate YBa₂(Cu_{1-y}Co_y)₃O_{7+ δ} (y=0.013, T_c =93 K). The observed structure factors differ slightly from that for the Cu(2) spins in the undoped state of the cuprates. This difference, observed in a sample where the doping level is high enough to support an optimum T_c value, questions the conclusion that a similar observation in well underdoped YBa₂Cu₃O_{6.6} is evidence for the predicted DDW order in the pseudo-gap phase. The cohabitation of AF and SC can be described as a formation of an AF phase within a d-wave superconductor. Whatever the precise mechanism giving rise to the AF ordering, our results reveal that hole-doped CuO₂ plane is close to an AF instability even when T_c remains optimum.

We wish to thank Pierre Gautier-Picard and Philippe Mendels for fruitful discussions.

- [1] N. D. Mathur et al., Nature **394**, 39 (1998).
- [2] A. Amato, Rev. Mod. Phys. 69, 1119 (1997).
- [3] Y.S. Lee et al., Phys. Rev. B 60, 3643 (1999).
- [4] J.M. Tranquada et al., Phys. Rev. B 59, 14712 (1999).
- [5] Y. Sidis et al., Phys. Rev. Lett. 86 4100 (2001).
- [6] H.A. Mook et al., Phys. Rev. B 64, 012502 (2001).
- [7] S. Chakravarty et al., Phys. Rev. B 63, 094503 (2001).
- [8] H. Kohno et al., J. Phys. Soc. Jpn., 68, 1500 (1999).
- [9] J.M. Tarascon et al., Phys. Rev. B 37, 7458 (1988).
- [10] R. S. Howland et al., Phys. Rev. B 39, 9017 (1989).
- [11] F. Bridges et al., Phys. Rev. B 39, 11603 (1989).
- [12] H. Renevier et al., Physica C 220, 143 (1994); Physica C 230, 31 (1994).
- [13] W.W. Schmahl et al., Phil. Mag. Lett. 60, 241 (1989).
- [14] R. Dupree et al., Physica C 193, 81 (1992).
- [15] J. Clayhold et al., Phys. Rev. B 39, 777 (1989).
- [16] J.W. Loram *et al.*, Supercond. Sci. Technol. 4, S184 (1991).
- [17] M. Matsumura et al., J. Phys. Soc Japan 63, 2382 (1994).
- [18] C. Vaast et al., Phys. Rev. B 56, 7886 (1995).
- [19] I. Mirebeau, et al., Phys. Rev. B 50, 3230 (1994).
- [20] H. Casalta, et al., Phys. Rev. B 50, 9688 (1994); E. Brecht, et al., Phys. Rev. B 52, 9601 (1995).
- [21] P. Zolliker, et al., Phys. Rev. B 38, 6575 (1988).
- [22] C. Bellouard et al., J. Mag. Mag. Mat. 104-107 517 (1992)
- [23] J. Rossat-Mignod et al. Physica C, 185-189, 86 (1991).
- [24] P. Bourges et al., Phys. Rev. B, 53, 876 (1996).
- [25] H.F. Fong, et al, Phys. Rev. B 61, , 14773 (2000).
- [26] Y. Sidis, et al, Phys. Rev. Lett. 84, , 5900 (2000).
- [27] Y. Ohashi et al., Phys. Rev. B 60, 15388 (1999).